Proc. Natl. Acad. Sci. USA
Vol. 85, pp. 9086–9090, December 1988
Cell Biology

Defining cellular senescence in IMR-90 cells: A flow cytometric analysis

STEVEN W. SHERWOOD*, DAPHNE RUSH, JEFFREY L. ELLSWORTH, AND ROBERT T. SCHIMKE

Department of Biological Sciences, Stanford University, Stanford, CA 94305

Contributed by Robert T. Schimke, September 12, 1988

ABSTRACT **Using multiparameter flow cytometric analysis, we find that senescent cells accumulate in a unique cell-cycle compartment characterized in cell-cycle arrest in G_1 and a significantly reduced nucleocytoplasmic ratio (genome size/cell mass) relative to cycling cells. With respect to gross cellular phenotype, the quiescent state of senescent cells differs from quiescence induced by density inhibition; the former is associated with a reduction in the nucleocytoplasmic ratio, while the latter is associated with an increase in the nucleocytoplasmic ratio. Senescent cells were present at all passages examined. The frequency of senescent cells was low in early-passage cultures and increased with passage number. Senescence of populations of IMR-90 cells reflects change in the relative frequency of these cells. The frequency of cells with karyotypic changes increased with the progressive accumulation of out-of-cycle cells.**

Human diploid fibroblast cells display the phenomenon of cellular senescence and have frequently been used as a model system to study *in vitro* cellular aging (1, 2). Senescence is defined as the loss of proliferative capacity of the cultures and results in the inability of the population to increase in cell number typically after cultures have been passaged 50 or more times. Senescence is associated with a number of gross cellular changes including cell-cycle arrest (3, 4), increase in cell size and size heterogeneity (5–8), and increase in the frequency of cells with chromosomal aberrations, including polyploidy (9–12). However, molecular data indicate that young and senescent cells do not consistently differ in the pattern of regulation of genes that are sensitive to serum stimulation (13) and several aspects of DNA replication have been reported not to change with culture age (14, 15). Thus, while senescent cells may retain normal DNA synthetic capacity, they fail to initiate DNA synthesis and the decline and finally loss of proliferative capacity involves alterations in some process(es) necessary for the initiation of DNA synthesis and/or cell-cycle progression.

We have examined the nature of the cell-cycle changes and correlated changes in the frequency of cells with karyotypic abnormalities occurring in IMR-90 cells (16) carried from passage 25 (young cells) to passage 53 (senescent cells). Using multiparameter flow cytometric analysis, we find an age-related increase in the frequency of cells that, based on DNA content, are blocked at the G_1/S (diploid and tetraploid) boundary but that become very large (>2 times the population mean) in size relative to cycling cells in the same cell-cycle phase. These large cells fail to label when grown in the presence of bromodeoxyuridine (BrdU) for up to 12 hr while small cells, even in late-passage cultures, do label. Senescent cells thus occupy a unique cell-cycle compartment definable on the basis of altered cell-cycle progression and nucleocytoplasmic ratio. Karyotypic changes associated with cellular aging induced an increase in the frequency of aneuploid and polyploid cells as well as chromosomal aberrations.

MATERIALS AND METHODS

Cell Culture. Passage 23 IMR-90 cells received from Gretchen Stein (University of Colorado) were maintained in 45% alpha-MEM/45% Ham's F-12 medium/10% fetal bovine serum (GIBCO) supplemented with 2 mM glutamine and penicillin/streptomycin. Cultures were grown in a 5% CO_2/95% air atmosphere. Early-passage cells were split 1:4 twice weekly. Midpassage cells were split 1:2 weekly and late-passage cultures were split 1:2 once cultures attained confluence. Culture medium was changed two or three times between subculture.

Flow Cytometry. Ethanol-fixed IMR-90 cells were analyzed for cellular DNA content after propidium iodide staining and cell size measurement (measured as 90° and forward-angle light scatter). The 90° light scatter (90LS) is well correlated with total protein content in ethanol-fixed cells and was routinely used for cell size measurement (S.W.S., unpublished data). Similar results were obtained with forward-angle light scatter, and light scatter measurements were corroborated by measurements of cell volume with a cell counter and Channelyzer (Coulter). To analyze the cell-cycle distribution of IMR-90 populations, cultures were labeled for 1–12 hr with 20 μM BrdU, chased for 15–30 min with 20 μM thymidine, and cells were fixed in 70% ethanol. Fixed cells were stained with a monoclonal antibody to BrdU (Beckton Dickinson) according to the method of Dolbeare *et al.* (17). Listmode data were collected and analyzed simultaneously for DNA content (propidium iodide), BrdU content (fluorescein fluorescence), and cell size (light scatter). Flow cytometry was performed on a Coulter EPICS 753 flow cytometer, and the data were processed on the Easy 88 computer system (Coulter).

Karyotype Analysis. Metaphase chromosomes were prepared from IMR-90 cells grown on glass coverslips. Cells were treated for 2–4 hr with Colcemid (GIBCO), treated with hypotonic solution (75 mM KCl), fixed with methanol/acetic acid (3:1), and stained on the coverslip with Giemsa. This procedure permitted examination of metaphase spreads without necessitating treatment of cells with trypsin. Cells were scored for the presence of chromosomal aberrations (18), aneuploidy, polyploidy, and the presence of micronuclei (19).

RESULTS

Flow Cytometric Analyses. Single parameter histograms of DNA content and 90LS for cells at passages 28, 36, and 53 are shown in Fig. 1. DNA histograms display an increase in the variability in both the G_1 and G_2/M peaks. The coefficient of variation for the G_1 peak increases from 5.4 in passage 28 cells to 10.2 in passage 53 cells, while the coefficient of

The publication costs of this article were defrayed in part by page charge payment. This article must therefore be hereby marked "*advertisement*" in accordance with 18 U.S.C. §1734 solely to indicate this fact.

Abbreviations: BrdU, bromodeoxyuridine; 90LS, 90° light scatter.
*To whom reprint requests should be addressed.

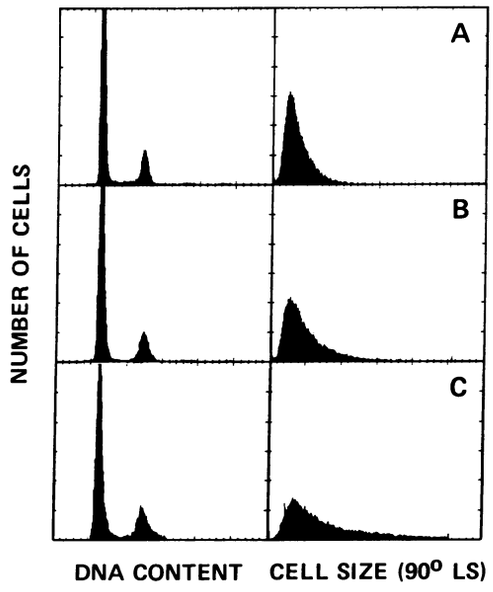

FIG. 1. Frequency histograms of fixed IMR-90 cells analyzed for cellular DNA content (*Left*) and cell size (*Right*). (*A*) Passage 23 cells. (*B*) Passage 36 cells. (*C*) Passage 53 cells. Each histogram represents 2×10^4 cells.

variation for the G_2/M peak increases from 5.2 in passage 28 cells to 7.6 by passage 53. The increased variability in DNA content of G_1 and G_2/M cells reflects in part an increase in the frequency of hypodiploid cells (Table 1) as well as an increase in the frequency of cells that are arrested at the G_1/S boundary. Cells with a DNA content of G_2/M cells typically represented 10–20% of the total number of cells present in late-passage cells. As discussed below, karyotypic analysis revealed that the frequency of tetraploid cells increased to ≈20% of the cell population in late-passage culture, and, therefore, the peak with G_2/M DNA content in late-passage cultures contains a significant number of G_1 tetraploid cells.

We used 90LS to measure cell size, which we found to be closely correlated with cell size, measured as total cellular protein by the Bradford assay (20) in ethanol-fixed cells. The cell size distributions show an age-related increase in both mean cell size and population variability, as shown in Fig. 1. The mean of the distributions is 35.4, 48.9, and 67.6 for passages 28, 36, and 53, respectively, while the coefficient of variation increased from 53 at passage 28 to 72 by passage 53. The increase in the population mean was associated with an increase in the frequency of very large cells, defined here as being >2 times the population mean, and also with an increase in the population mode (Fig. 1). While the size distribution of late-passage cultures increases significantly, small cells comprise a significant proportion of the cell population even in late-passage cultures (Figs. 1 and 2).

When cell size and cellular DNA content were examined simultaneously, the increased variability in cell size in senescing cell populations was seen to result from the development of subpopulations of very large cells with both G_1 and G_2/M DNA content (Fig. 2). Large G_1-arrested cells in late-passage populations equaled or exceeded the size of cycling G_2/M cells. For cell populations fixed at similar times after plating (6–8 days), the relative proportion of the total cell population represented by this subpopulation progressively increased with passage number (Fig. 2). Large G_1 cells were present even in early-passage cultures (<5%), but their frequency increased, and by passage 50 these cells typically represented >25% of the total cell population (Fig. 2). For the latest-passage cells shown (passage 53), the mean cell size of the total population of cells with a G_1 DNA content was 2 times that of the G_1 population in passage 28 cells, reflecting the accumulation of these large cells.

Table 1. Frequency of IMR-90 cells with various forms of karyotypic abnormality

Passage	Hypodiploid	Polyploid	Micronuclei	Aberrations
23–28	0.039	0.040	0.005	0.029
31, 33	0.086	0.050	0.010	0.052
42, 49	0.111	0.120	0.012	0.060
54, 55, 57	0.145	0.220	0.083	0.196

A minimum of 130 cells was scored per passage, and numbers represent the mean for the passages shown. Aberrations include chromosome and chromatid breaks and gaps, complex exchange figures, dicentric chromosomes, and chromosomal fragments.

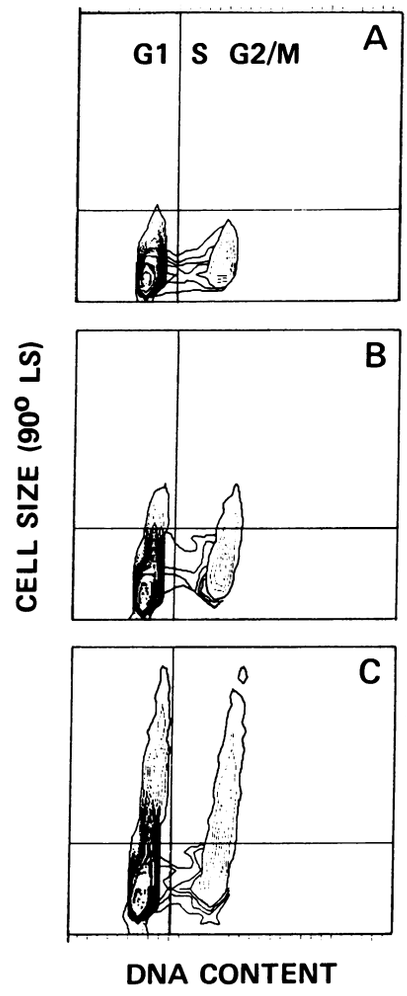

FIG. 2. Correlated two-parameter frequency histograms for IMR-90 cells at passages 23 (*A*), 36 (*B*), and 53 (*C*). DNA content is shown on the *x* axis and cell size (90LS) is on the *y* axis. Cell frequency is on the *z* axis and is shown as 5% contour intervals. Horizontal and vertical markers were set to partition G_1 cells into "large" and "small" classes.

The histograms in Fig. 2 also show that while the frequency of S-phase cells decreases in late-passage cultures, the size of S-phase cells did not increase with passage number as it did for the population as a whole. This observation suggests that actively cycling cells remain "normal" in size in late-passage cultures and that aging cell populations become functionally bimodal with actively proliferating cells remaining relatively small in size and out-of-cycle (senescent) cells arresting in G_1 and becoming "abnormally" large.

To examine this further, we treated late-passage cultures with BrdU to label S-phase cells and, using gated multipa-

rameter analysis, determined that the large cells do not incorporate BrdU. This is shown in Fig. 3 for passage 50 cells labeled for 1.5 hr with 20 μM BrdU and chased for 30 min with 20 μM thymidine. In this figure, the first panel in each row presents the size distribution of the entire cell population (90LS), which as in Fig. 1 shows the long "tail" of very large cells that become increasingly abundant as cultures age. The second and third panels show, respectively, the DNA vs. cell size and DNA vs. BrdU content distributions of the shaded portion of the size distributions shown in the first panel. The G_1, S, and G_2/M fractions of the total population are clearly seen in the DNA vs. BrdU distributions, and it is apparent that when only the very large cells are examined (shaded areas in the third row of figures), no S-phase cells are present. Identical results were obtained with populations at all passage levels with labeling times up to 12 hr. Longer labeling times have not been used because of the cell-cycle perturbing effects of BrdU. With 12 hr of labeling, it was possible to observe labeled cells proceed through mitosis into a second S phase, while large cells failed to label (proceed into S phase). Thus, in late-passage cultures, a subpopulation of relatively small cells continues to progress into and through S phase, while the very large cells are noncycling (i.e., cells that do not incorporate BrdU). A small subpopulation (<5%) of nonlabeling large cells (noncycling) was also observed in early-passage (passage 23) cultures and appears to represent "senescent" cells.

Karyotypic Changes in IMR-90 Cells. Chromosome analysis was used to assess the degree of genomic instability associated with *in vitro* aging in IMR cells. The frequency of cells that deviated from the diploid chromosome number ($2n$ = 46) increased with culture age as shown in Table 1. In early-passage (<30) cultures, >92% of the cells had a normal diploid number of chromosomes. Of the remaining cells, 3–4% were hypodiploid and 4–5% were tetraploid. Both hypodiploidy and tetraploidy increased steadily with passage number, as shown in Table 1, generally paralleling the increased heterogeneity of the cell populations with respect to cell size measured by flow cytometry.

In contrast to the pattern of gradual increase in the frequency of cells with numerical variation in the karyotype, the frequency of cells with actual chromosome damage remained relatively stable until very late passages, at which time there was a sudden increase in the frequency of cells with damaged chromosomes. The presence of micronuclei (an indirect but well-characterized measure of chromosome damage) showed little change in frequency in cultures from passages 23–49. In very late-passage cultures, however, the frequency of cells with micronuclei increased to ≈8-fold the level of early-passage cells. When chromosome damage (chromosomal and chromatid breaks, gaps, exchange figures, fragments, and dicentric chromosomes) was examined directly in metaphase spreads, the frequency of cells with aberrant metaphase chromosomes increased slowly up to a

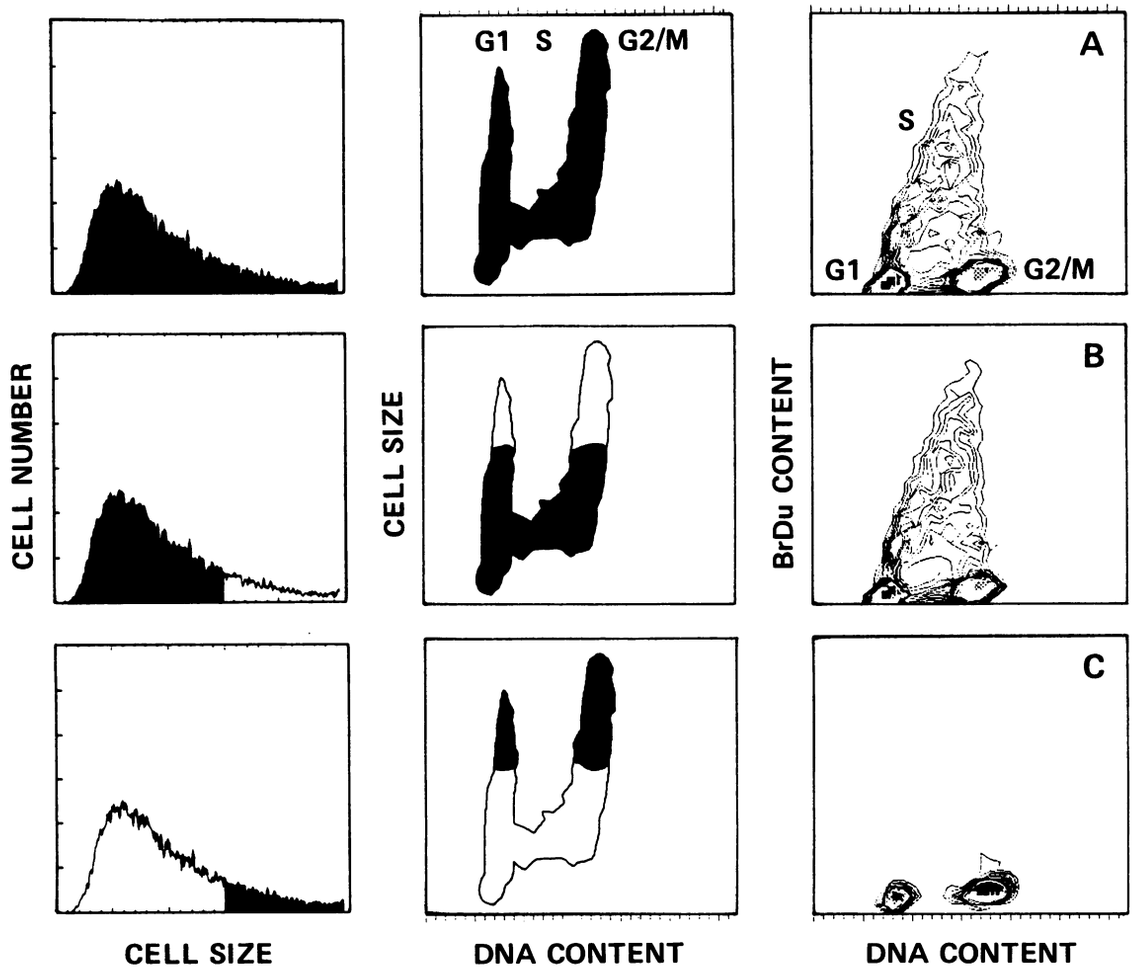

FIG. 3. Multiparameter analysis of passage 53 IMR-90 cells. BrdU-labeled cells were simultaneously analyzed for DNA content (PI), BrdU content (anti-BrdU monoclonal antibody), and cell size (90LS). The first panel in each row represents the size distribution of the cell population. The second panel shows DNA content (x axis) vs. cell size (y axis), and the third panel shows DNA content (x axis) vs. BrdU content (y axis). The latter two histograms are derived solely from the shaded portion of the size distribution shown in the first panel of each row.

late-passage number, at which time the frequency increased sharply (Table 1). Thus, two patterns of chromosomal change were apparent in IMR-90 cells, a gradual increase in the frequency of cells with numerical chromosome variation that paralleled the changes in cell population with respect to the frequency of out-of-cycle cells and an increase in chromosome damage that occurred in very late-passage cells.

DISCUSSION

The concept of cellular senescence is used in two ways: (*i*) to describe entire cultures in which case the meaning of senescence relates to the decrease in proliferative potential of the culture and is measured as the decline in the frequency of cells that can divide; (*ii*) to describe the phenotype of the cells that are responsible for the decline in proliferative potential of aging cell populations. The phenotype of senescent cells is usually defined with respect to the decreased ability of aging cells to replicate DNA. Our studies show that out-of-cycle (senescent) cells can be defined on the basis of gross cell size and cell-cycle position and that senescence in aging cell populations reflects the accumulation of cells in this cell-cycle compartment.

Using multiparameter flow cytometry, we find that noncycling IMR-90 cells accumulate in a distinct cell-cycle compartment characterized by a G_1 (diploid and tetraploid) DNA content and a low nucleocytoplasmic ratio (very large cell size) relative to cells that continue to cycle. We define nucleocytoplasmic ratio as the ratio of cellular DNA content (G_1, S, or G_2/M DNA content) to total cell mass, rather than the ratio of nuclear mass to cytoplasmic mass. We find that senescent cells are present even in early-passage cultures (passage 23) but comprise <5% of the total population. The frequency of cells in this compartment increases steadily with passage level and is directly related to declining proliferative potential of senescing cultures of IMR-90 cells. Using BrdU labeling and subsequent staining with an anti-BrdU monoclonal antibody, we have established directly that cycling cells, even in late-passage cultures, remain of normal size and that the large cells (>2 times the population mean) that accumulate in senescing cultures do not cycle (i.e., enter S phase as measured by BrdU incorporation into DNA). In cell populations labeled for up to 12 hr, we have never observed labeling in the large cells. Thus, while the cell size distribution of IMR-90 cell populations shows an age-related increase in both mean cell size (90LS and cell volume) and size variability consequent to the accumulation of large out-of-cycle cells, the population remains functionally bimodal, being comprised of actively cycling (small) cells, and viable, though nonclonogenic (senescent), large cells (6, 21). Senescence of IMR-90 cell populations reflects the progressive change in the relative proportion of these two components of the cell population (22).

The relationship of cellular quiescence to senescence has received considerable discussion but remains unresolved (23–25). Quiescence in which cells enter G_0 results in a reversible block in cell-cycle progression in cells with a G_1 DNA content. In this type of quiescence, the cessation of cellular growth is coupled to the cessation of cell-cycle progression and hence quiescent cells usually are smaller in size than cycling G_1 cells, reflecting a reduction in cellular RNA and protein content (26). Senescent cells have been reported to be blocked in G_1 or at the G_1/S boundary, and, as shown here, the majority (>90%) of the cells in late-passage IMR-90 cultures have a DNA content of G_1 and G_2/M cells. We infer from direct counts of tetraploid cells in senescing cultures that the majority of the cell population with a G_2/M DNA content represents G_1 tetraploid cells, although we cannot discount the possibility that some cells with G_2/M DNA content are senescent cells arrested in G_2. However, as previously reported (8) and shown directly here, senescent cells, while blocked in G_1, are larger in size than cycling G_1 cells and senescent cells "exit" from the cell cycle with a nucleocytoplasmic ratio lower than actively cycling G_1/S cells. Thus, cellular senescence involves processes that result in an imbalance in the integration of cell growth with cell-cycle progression, and, in this sense, cellular senescence differs significantly from quiescence. As shown here, senescent cells differ from cycling G_1 cells in nucleocytoplasmic ratio, even though late-passage cells retain certain characteristics of younger cells, including the serum-inducible expression of several genes normally associated with cell-cycle progression and entry into S phase (13). Senescence, therefore, represents a specific type of quiescence distinct from G_0 arrest. This feature of senescent cells is reminiscent of unbalanced cellular growth, which has been shown in *Escherichia coli* (27) and mammalian cells (28) to be associated with chromosomal aberrations and cell death when cells proceed through the cell cycle. While the relationship between altered nucleocytoplasmic ratio and cessation of cell-cycle traverse remains to be clarified, we suggest that senescence involves an alteration of the integration of cell growth and cell-cycle progression more extensive than a "simple" failure of cells to initiate DNA synthesis.

We observed two patterns of age-related change in the karyotype of IMR-90 cells. Overall, numerical variation—i.e., aneuploidy and polyploidy—increased gradually with passage number, paralleling the progressive change in the frequency of noncycling cells present in the population. While hypodiploidy increased relatively evenly over time, the frequency of polyploid cells increased most rapidly in very late-passage cultures (Table 1). The fact that we did not observe an increase in hyperdiploid cells suggests that hypodiploidy does not result from nondisjunction but represents chromosome loss occurring by some other mechanism. This needs to be examined further. In any event, numerical variation in the karyotype of IMR-90 cells is associated with cell-cycle changes, perhaps reflecting mitotic instability consequent to altered cell-cycle progression (3). It is also possible that chromosome loss may be a relatively early event in senescence and that alterations in cell-cycle progression might then reflect loss or imbalance in specific DNA sequences. In either case, karyotypic instability and changes in cell-cycle progression, as shown recently in mouse fibroblasts (29), appear to be related aspects of cellular senescence.

We thank Dr. Gretchen Stein for the gift of IMR-90 cells. This work was supported by National Institutes of Health Grants GM-14931 and AG-05568.

1. Hayflick, L. & Moorhead P. S. (1961) *Exp. Cell Res.* **25,** 585–621.
2. Hayflick, L. (1965) *Exp. Cell Res.* **37,** 614–636.
3. Yanishevsky, R., Mendelsohn, M. L., Mayall, B. H. & Cristafalo, V. J. (1974) *J. Cell. Physiol.* **84,** 165–170.
4. Yanishevsky, R. & Carrano, A. V. (1975) *Exp. Cell Res.* **90,** 169–174.
5. Bowman, P. D., Meek, R. L. & Daniels, C. W. (1975) *Exp. Cell Res.* **93,** 184–190.
6. Houghton, B. A. & Stidworthy, G. H. (1979) *In Vitro* **15,** 697–702.
7. Mitsui, Y. & Schneider, E. L. (1976) *Exp. Cell Res.* **100,** 147–152.
8. Schneider, E. L. & Fowlkes, B. J. (1976) *Exp. Cell Res.* **98,** 298–302.
9. Sax, H. J. & Passano, N. K. (1961) *Am. Nat.* **45,** 97–102.
10. Saksela, E. & Moorhead, P. S. (1963) *Proc. Natl. Acad. Sci. USA* **50,** 390–395.
11. Benn, P. A. (1976) *Am. J. Hum. Genet.* **28,** 465–473.
12. Thompson, K. V. A. & Holliday, R. (1975) *Exp. Cell Res.* **96,** 1–6.

13. Rittling, S. R., Brooks, K. M., Cristafalo, V. J. & Baserga, R. (1986) *Proc. Natl. Acad. Sci. USA* **83,** 3316–3320.
14. Hasegawa, N., Hanaoka, F., Hori, T. & Yamada, M. (1982) *Exp. Cell Res.* **140,** 443–450.
15. Hasegawa, N., Hanaoka, F. & Yamada, M. (1985) *Exp. Cell Res.* **156,** 468–486.
16. Nichols, W. W., Murphy, D. G., Cristafalo, V. J., Toji, L. H., Greene, A. E. & Dwight, S. A. (1977) *Science* **196,** 60–63.
17. Dolbeare, F., Gratzner, H., Pallavacini, M. & Gray, J. W. (1983) *Proc. Natl. Acad. Sci. USA* **80,** 5573–5577.
18. Standing Committee on Human Cytogenetic Nomenclature (1970) *Cytogenet. Cell Genet.* **21,** 309–404.
19. Heddle, J. A., Hite, M., Kirkhart, B., Mavournin, K., MacGregor, J. T., Newell, G. W. & Salamone, M. F. (1983) *Mutat. Res.* **123,** 61–118.
20. Bradford, M. (1976) *Anal Biochem.* **72,** 248–254.
21. Angelo, J. C., Pendergrass, W. P., Norwood, T. H. & Prothero, J. (1987) *J. Cell. Physiol.* **132,** 125–130.
22. Rabinovitch, P. S. (1983) *Proc. Natl. Acad. Sci. USA* **80,** 2951–2955.
23. Periera-Smith, O. M., Fisher, S. F. & Smith, J. R. (1985) *Exp. Cell Res.* **160,** 297–306.
24. Stein, G. H., Namba, M. & Corsaro, C. M. (1985) *J. Cell. Physiol.* **122,** 343–349.
25. Stein, G. H. & Atkins, L. (1986) *Proc. Natl. Acad. Sci. USA* **83,** 9030–9034.
26. Darzynkiewicz, Z. (1986) in *Techniques in Cell Cycle Analysis*, eds. Gray, J. W. & Darzynkiewicz, Z. (Humana, Clifton, NJ), pp. 255–290.
27. Pritchard, R. H. & Clark, K. G. (1964) *J. Mol. Biol.* **9,** 288–307.
28. Sherwood, S. W., Schumacher, R. I. & Schimke, R. T. (1988) *Mol. Cell. Biol.* **8,** 2822–2827.
29. Loo, D. T., Fuguay, J. I., Dawson, C. L. & Barnes, D. W. (1987) *Science* **236,** 200–202.